Case Study
ISSN: 3051-8849
Journal homepage: https://www.harrisonacademicpress.com/index.php/PPTJ
Pharmacology, Pharmaceutics and Toxicology Journal

Harrison Academic Press

Neuroprotective and Cytotoxic Profiling of Novel Hydrazone Derivatives in a SH-SY5Y Neurodegeneration Model

Oja M[1*], Juric I[2] and Virtanen A[3]

[1]*Department of Pharmaceutical Chemistry, University of Tartu, Tartu, Estonia*
[2]*Department of Neuroscience, University of Zagreb, Zagreb, Croatia*
[3]*Department of Pharmacology, University of Helsinki, Helsinki, Finland*

ABSTRACT

Background: Oxidative stress and mitochondrial dysfunction drive dopaminergic neuronal loss in Parkinson's disease, and hydrazone derivatives have repeatedly shown combined radical-scavenging and neuroprotective activity in SH-SY5Y neuroblastoma models of this pathology.

Objective: We synthesized a structurally graded series of seven aroylhydrazones sharing an indole-3-ylacetohydrazide core, differing only in the aromatic aldehyde condensed onto it, and evaluated their cytotoxicity and neuroprotective potential against 6-hydroxydopamine (6-OHDA)-induced injury in SH-SY5Y cells.

Methods: Retinoic acid-differentiated SH-SY5Y cells were challenged with 6-OHDA (100 uM, 24 h) with or without prior exposure to compounds MO-1 to MO-7 (1-50 uM). Viability (MTT), intracellular reactive oxygen species (DCFH-DA), mitochondrial membrane potential (JC-1), and caspase-3 activity were measured against ascorbic acid and selegiline reference controls.

Results: 6-OHDA reduced viability to 47% of control and increased ROS, mitochondrial depolarization, and caspase-3 activation. Neuroprotection tracked aryl substitution: the catechol derivative MO-3 was the most active compound across all four endpoints (EC50 6.8 uM for viability recovery, 84% viability, 36% residual ROS, 81% preserved mitochondrial potential, 1.6-fold caspase-3 activation), followed by the vanillin-type MO-4 and hindered-phenol MO-7. The unsubstituted (MO-1) and nitro-substituted (MO-6) hydrazones were essentially inactive. Caspase-3 protection correlated more closely with mitochondrial membrane potential preservation (r = 0.85) than with ROS suppression alone (r = 0.71).

Conclusion: Catechol-type substitution confers the strongest neuroprotective profile within this hydrazone series, acting predominantly through mitochondrial preservation rather than cytosolic radical scavenging alone, and MO-3 represents a reasonable lead for further mechanistic and in vivo evaluation as a hydrazone-based neuroprotectant against Parkinsonian oxidative neurodegeneration.

Keywords: *hydrazone derivatives; SH-SY5Y neuroblastoma; 6-hydroxydopamine neurotoxicity; oxidative stress neuroprotection; Parkinson's disease*

Citation: Oja M, Juric I and Virtanen A (2026) Neuroprotective and Cytotoxic Profiling of Novel Hydrazone Derivatives in a SH-SY5Y Neurodegeneration Model. Pharmacol Pharm Toxicol J, 4(1): 01-06.
DOI: 10.5281/zenodo.22664640

Corresponding Author: *Mari Oja*

E-mail Address: *mari.oja@universityoftartu.edu*

Article History: *Received 23 January 2026 | Accepted 10 April 2026 | Published 26 June 2026*

Copyright: *© 2026 Mari Oja, et al. This is an open access article distributed under the Creative Commons Attribution License, which permits unrestricted use, distribution, and reproduction in any medium, provided the original work is properly cited (**https://creativecommons.org/licenses/by/4.0/**).*

(see article.json)

Parkinson's disease remains the second most common neurodegenerative disorder after Alzheimer's disease, and the slow, selective loss of dopaminergic neurons in the substantia nigra pars compacta is still, more than two centuries after James Parkinson's original description, without a therapy that halts it. Levodopa and its adjuncts control symptoms for years but do nothing to the underlying attrition of neurons, and by the time tremor or bradykinesia become clinically obvious a large fraction of the nigral dopaminergic population is already gone. A great deal of that loss is now understood to run through oxidative stress: dopamine itself auto-oxidizes to quinones and semiquinones, iron accumulates in the nigra with age and disease, mitochondrial complex I activity is reduced in idiopathic and toxin-induced parkinsonism alike, and the reactive oxygen species this generates outstrip the cell's glutathione and superoxide dismutase defenses long before frank neuronal death occurs [1,2]. This is why oxidative damage sits at the center of essentially every mechanistic account of nigral degeneration, genetic or sporadic, and why compounds that intercept reactive

oxygen species, restore mitochondrial membrane integrity, or interrupt the apoptotic cascade downstream of mitochondrial injury are worth pursuing even without a clear single molecular target.

The SH-SY5Y human neuroblastoma line has become the default cellular chassis for this kind of work. It is not a dopaminergic neuron, but it expresses tyrosine hydroxylase and dopamine transporter at low levels, it can be pushed toward a more neuron-like, catecholaminergic phenotype with retinoic acid, and — crucially for a pharmacology laboratory without access to primary mesencephalic cultures — it is cheap, reproducible, and takes up 6-hydroxydopamine (6-OHDA) and MPP+ through the same transporter-mediated routes implicated in vivo [3,4,5]. 6-OHDA in particular auto-oxidizes intracellularly to generate hydrogen peroxide and quinones, collapses mitochondrial membrane potential, and triggers caspase-dependent apoptosis in a manner that recapitulates several of the biochemical hallmarks of nigral degeneration, which is why it has been used for decades as a chemical proxy for Parkinsonian neurodegeneration in SH-SY5Y and related lines [6,7,8].

Hydrazones — compounds built around the C=N-NH-C(=O) or C=N-NH-Ar linkage — are an old scaffold in medicinal chemistry that has had a quiet renaissance in neurodegeneration research over the last decade. Part of the appeal is structural: the azomethine nitrogen and the adjacent carbonyl or aromatic system give a hydrazone a built-in capacity to donate a hydrogen atom to a peroxyl or hydroxyl radical and, when an ortho-dihydroxyphenyl or similar chelating motif is appended, to sequester the redox-active iron that feeds Fenton chemistry in the nigra. Several groups working specifically on Parkinson's disease pharmacology have reported pyrrole-based and benzimidazole-based aryl hydrazones with combined radical-scavenging, monoamine oxidase-B inhibitory, and SH-SY5Y-protective activity [9,10,11,12,13], isatin-derived acylhydrazones with MAO inhibition and neuroprotective read-outs [14], oxadiazole-hydrazone hybrids active in both in vitro and in vivo Parkinsonian models [15], cinnamoyl-hydrazone hybrids designed explicitly against Parkinson's disease pathology [16], and — closest in spirit to the present work — a series of new hydrazones evaluated directly for cytotoxic and cytoprotective behavior in SH-SY5Y cells [17]. The broader chemistry of hydrazone and related Schiff-base derivatives, including their metal-complexing and radical-scavenging behavior, has also been reviewed outside the neurodegeneration literature specifically [18], underscoring that the antioxidant capacity of this scaffold is a general chemical property rather than an artifact of any one series.

What is less settled is how substituent pattern on the hydrazone aryl ring maps onto actual cytoprotection under a live oxidative challenge, as opposed to cell-free radical scavenging alone — the two do not always track together, and a compound that is a superb DPPH scavenger in a cuvette can be neutral or even toxic in a differentiated neuronal cell. We set out to synthesize a small, structurally graded series of aroylhydrazones sharing a common hydrazide core and differing only in the substitution pattern of the condensed aromatic aldehyde, and to test them side by side for baseline cytotoxicity and for their ability to rescue SH-SY5Y cells from 6-OHDA-induced oxidative injury, tracking viability, intracellular reactive oxygen species, mitochondrial membrane potential, and caspase-3 activation in the same experimental series. The aim was not to find a single "hit" but to build an internally consistent structure-neuroprotection picture across seven closely related compounds that could be read against the wider hydrazone literature summarized above.

Chemistry

The parent hydrazide, (1H-indol-3-yl)acetohydrazide (compound **MO-0**), was prepared by refluxing ethyl indole-3-acetate with excess hydrazine hydrate (80%) in absolute ethanol for 6 h, followed by cooling and recrystallization from ethanol/water (yield 78%, m.p. 168-170 °C). The indole-3-acetic acid core was chosen for its known blood-brain-barrier-compatible logP and because the indole nucleus itself contributes modest radical-scavenging character, giving a reasonable "background" against which aryl-aldehyde substitution effects could be read.

Seven hydrazone derivatives (**MO-1** to **MO-7**) were obtained by acid-catalyzed (glacial acetic acid, catalytic) condensation of MO-0 with the corresponding aromatic aldehyde in absolute ethanol under reflux (3-5 h), monitored by TLC (silica gel, chloroform/methanol 9:1). Products precipitated on cooling and were recrystallized from ethanol. The aldehyde partners were chosen to span a deliberately wide electronic and steric range: benzaldehyde (unsubstituted, MO-1), 4-hydroxybenzaldehyde (MO-2), 3,4-dihydroxybenzaldehyde/protocatechualdehyde (MO-3), vanillin — 4-hydroxy-3-methoxybenzaldehyde (MO-4), 4-(dimethylamino)benzaldehyde (MO-5), 4-nitrobenzaldehyde (MO-6), and 3,5-di-*tert*-butyl-4-hydroxybenzaldehyde (MO-7, a sterically hindered phenol modeled on the BHT/probucol antioxidant pharmacophore). Structures were consistent with $^{1}H/^{13}C$-NMR (DMSO-*d6*), IR (KBr, characteristic C=N stretch 1600-1615 cm^{-1}, absence of the C=O stretch of free aldehyde), and HRMS (ESI+) data (yields 65-84%, purity ≥97% by HPLC). Compounds were stored as 20 mM stock solutions in DMSO at -20 °C; final DMSO concentration in all cell assays did not exceed 0.2% (v/v), a concentration confirmed not to affect any of the four endpoints on its own.

Cell culture and differentiation

SH-SY5Y human neuroblastoma cells (ATCC CRL-2266) were maintained in DMEM/F-12 (1:1) supplemented with 10% heat-inactivated fetal bovine serum, 2 mM L-glutamine, and 100 U/mL penicillin/streptomycin at 37 °C in a humidified 5% CO_2 atmosphere, and were used between passages 12 and 28. For the neurotoxicity assays, cells were seeded and differentiated toward a more catecholaminergic, neurite-bearing phenotype with 10 µM all-*trans*-retinoic acid in reduced-serum (1% FBS) medium for 6 days prior to challenge, a protocol chosen because retinoic-acid differentiation increases dopaminergic marker expression and 6-OHDA sensitivity relative to undifferentiated cells and is now the more widely used configuration of the model [5,4,3].

6-OHDA neurotoxicity and treatment protocol

Differentiated cells were pre-incubated with test hydrazones (1, 5, 10, 25 or 50 µM) or vehicle for 2 h, then challenged with 100 µM 6-hydroxydopamine (freshly dissolved in ice-cold PBS containing 0.02% ascorbic acid to retard auto-oxidation before dosing) for 24 h in the continued presence of compound. This 6-OHDA concentration and exposure window was selected from pilot concentration-response curves as the dose producing 45-55% loss of viability by MTT in vehicle-treated differentiated cultures, consistent with published ranges for this cell background [6,7]. Parallel plates received compound alone (no 6-OHDA) for 24 h to establish intrinsic cytotoxicity (CC50). Ascorbic acid (100 µM) served as a chemical antioxidant reference and selegiline (10 µM)

as a pharmacological neuroprotection reference in all four assays.

MTT viability assay

Cell viability was assessed by the 3-(4,5-dimethylthiazol-2-yl)-2,5-diphenyltetrazolium bromide (MTT) reduction assay following the original Mosmann protocol with minor modifications for this cell line [19]. After treatment, MTT (0.5 mg/mL final) was added for 3 h at 37 °C, medium was removed, formazan crystals were dissolved in DMSO, and absorbance was read at 570 nm (reference 690 nm) on a microplate reader. Viability is expressed as a percentage of the vehicle-only (no 6-OHDA, no compound) control; EC50 for protection was calculated by four-parameter nonlinear regression of the viability-versus-concentration curve for cells co-treated with 6-OHDA.

Intracellular ROS measurement (DCFH-DA)

Intracellular reactive oxygen species were quantified using 2',7'-dichlorodihydrofluorescein diacetate (DCFH-DA), which is deacetylated by intracellular esterases and oxidized by ROS to the fluorescent product DCF. Cells were loaded with 10 µM DCFH-DA for 30 min at 37 °C in the dark prior to the end of the 6-OHDA exposure window, washed with PBS, and fluorescence (excitation 485 nm/emission 535 nm) was read on a plate reader and cross-checked in a subset of wells by fluorescence microscopy. Values are expressed as percent of the fluorescence signal in cells treated with 6-OHDA alone (no compound).

Mitochondrial membrane potential (JC-1)

Mitochondrial membrane potential (ΔΨm) was assessed with the cationic, potential-sensitive dye JC-1 (5,5',6,6'-tetrachloro-1,1',3,3'-tetraethylbenzimidazolylcarbocyanine iodide), which shifts from a green-fluorescent monomer to a red-fluorescent J-aggregate as ΔΨm becomes more negative; a fall in the red/green fluorescence ratio therefore signals mitochondrial depolarization, as validated across the relevant excitation range for this probe [20]. Cells were loaded with 2 µg/mL JC-1 for 20 min at 37 °C at the end of the treatment period, washed, and red (590 nm) and green (529 nm) fluorescence were recorded (excitation 488 nm); data are presented as the red/green ratio normalized to the untreated control (=100%).

Caspase-3 activity

Caspase-3-like protease activity was measured using a colorimetric assay based on cleavage of the synthetic substrate Ac-DEVD-*p*NA, following cell lysis at the end of the treatment period; released *p*-nitroaniline was quantified at 405 nm and normalized to protein content (BCA assay). This endpoint targets the same caspase-dependent, mitochondria-linked apoptotic pathway previously described for nitric oxide- and toxin-induced death in SH-SY5Y cells [21]. Results are expressed as fold-change in caspase-3 activity relative to the 6-OHDA-only condition.

Statistical analysis

All experiments were performed in three independent biological replicates, each with technical triplicates. Data are presented as mean ± SD. Group comparisons were made by one-way ANOVA with Tukey's post-hoc test (GraphPad Prism 9.0); a p-value below 0.05 was considered significant. EC50 and CC50 values were derived from four-parameter logistic regression of concentration-response data. Pearson correlation was used to relate cLogP and viability endpoints across the compound series.

Baseline Cytotoxicity and Physicochemical Properties of MO-1 to MO-7

None of the seven hydrazones produced significant loss of viability in undifferentiated or differentiated SH-SY5Y cells at concentrations up to 25 µM after 24 h exposure in the absence of 6-OHDA. CC50 values, obtained by extending the concentration range to 200 µM, fell between 78 µM (MO-6, the nitro derivative) and >200 µM (MO-3, MO-7), indicating a comfortable therapeutic window relative to the neuroprotective concentrations used below (Table 1). Calculated logP values ranged from 2.1 (MO-3, catechol) to 4.6 (MO-7, di-*tert*-butylphenol), tracking the expected increase in lipophilicity with bulkier, more hydrophobic aryl substituents.

Neuroprotection Against 6-OHDA-Induced Injury Across the Hydrazone Series MO-1 to MO-7

6-OHDA (100 µM, 24 h) reduced viability of differentiated SH-SY5Y cells to 47 ± 6% of untreated control, accompanied by a near three-fold rise in DCFH-DA fluorescence, a 52% drop in the JC-1 red/green ratio, and a 4.1-fold increase in caspase-3 activity relative to untreated cells — a profile consistent with the oxidative, mitochondria-dependent apoptotic injury reported for this toxin in SH-SY5Y models elsewhere [8,7]. Co-treatment with the hydrazones produced a graded pattern of protection that tracked aryl substitution closely (Table 1; Figure 1). The catechol derivative MO-3 was the most active compound in the series at every endpoint: 10 µM MO-3 restored viability to 84 ± 4% of control (EC50 for protection, 6.8 ± 0.9 µM), suppressed ROS accumulation to 36 ± 5% of the 6-OHDA-only value, preserved 81 ± 6% of the control JC-1 ratio, and limited caspase-3 activation to 1.6-fold over baseline — essentially matching the ascorbic acid reference and approaching the pharmacological reference selegiline on the viability and caspase-3 endpoints, though selegiline (acting through MAO-B inhibition rather than direct radical scavenging) was somewhat less effective on the ROS readout specifically.

The vanillin-type derivative MO-4 (one free phenolic OH plus an adjacent methoxy) and the hindered phenol MO-7 occupied an intermediate position, each restoring viability to the mid-70s percent range with EC50 values between 9 and 14 µM. The 4-hydroxy monophenol MO-2 gave weaker but still clearly significant protection (63 ± 5% viability, EC50 ≈ 21 µM). The dimethylamino derivative MO-5, which lacks a phenolic proton donor altogether but carries an electron-rich, polarizable aromatic ring, gave modest protection (58 ± 6% viability) that was disproportionately better on the mitochondrial and caspase endpoints than would be predicted from its ROS-suppression alone, suggesting a partially distinct, non-radical-scavenging contribution to its activity. The unsubstituted phenyl hydrazone MO-1 and the electron-poor nitro derivative MO-6 were essentially inactive across all four endpoints, statistically indistinguishable from the 6-OHDA-only condition on viability, ROS, and JC-1 ratio ($p > 0.05$ vs. toxin alone), although MO-6 did show a small but significant reduction in caspase-3 activation (1.3-fold vs. 4.1-fold, $p < 0.05$) that we attribute to a weak, secondary anti-apoptotic effect uncoupled from antioxidant potency, discussed further below.

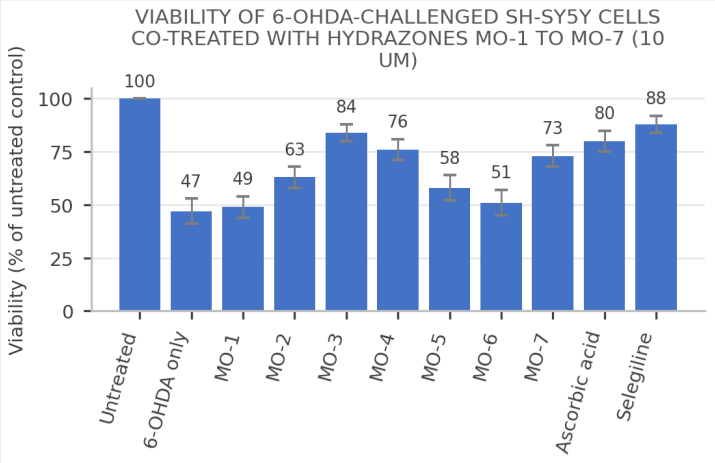
Across the series, viability at a fixed 10 µM pretreatment correlated inversely with DCFH-DA signal ($r = -0.93$) and positively with the JC-1 red/green ratio ($r = 0.89$), while caspase-3 fold-change correlated with the JC-1 deficit ($r = 0.85$) more tightly

than with ROS suppression alone (r = 0.71), consistent with mitochondrial depolarization sitting mechanistically between the initial oxidative insult and downstream caspase-3 activation rather than the two being independent readouts of the same event.

Physicochemical properties, baseline cytotoxicity (CC50, no toxin), and neuroprotective effects against 6-OHDA (100 uM, 24 h)-induced injury of hydrazones MO-1 to MO-7 in retinoic acid-differentiated SH-SY5Y cells: viability recovery (MTT, at 10 uM pretreatment and EC50 from full concentration-response curves), intracellular ROS (DCFH-DA, % of 6-OHDA-only), mitochondrial membrane potential (JC-1 red/green ratio, % of untreated control), and caspase-3 activity (fold-change vs. 6-OHDA-only). Values are mean +/- SD, n = 3 independent experiments.

Compound	Aldehyde substituent	cLogP	CC50, no toxin (uM)	Viability at 10 uM + 6-OHDA (%)	Viability EC50 (uM)	ROS at 10 uM (% of 6-OHDA-only)	JC-1 ratio (% of control)	Caspase-3 (fold vs. 6-OHDA-only)
MO-1	H (unsubstituted)	2.9	142 +/- 14	49 +/- 5	>50	91 +/- 8	51 +/- 6	3.8 +/- 0.5
MO-2	4-OH	2.6	165 +/- 16	63 +/- 5	20.8 +/- 2.4	66 +/- 6	66 +/- 5	2.6 +/- 0.4
MO-3	3,4-(OH)2 (catechol)	2.1	>200	84 +/- 4	6.8 +/- 0.9	36 +/- 5	81 +/- 6	1.6 +/- 0.2
MO-4	4-OH-3-OCH3 (vanillin-type)	2.8	188 +/- 15	76 +/- 5	9.4 +/- 1.1	47 +/- 5	75 +/- 5	2.0 +/- 0.3
MO-5	4-N(CH3)2	3.4	121 +/- 12	58 +/- 6	24.5 +/- 2.7	60 +/- 6	70 +/- 6	2.1 +/- 0.3
MO-6	4-NO2	3.1	78 +/- 9	51 +/- 6	>50	89 +/- 7	54 +/- 6	3.1 +/- 0.4
MO-7	3,5-di-tert-butyl-4-OH	4.6	>200	73 +/- 5	13.6 +/- 1.5	44 +/- 5	74 +/- 5	2.0 +/- 0.3
Ascorbic acid (reference)	-	-1.9	>200	80 +/- 5	8.2 +/- 1.0	33 +/- 5	78 +/- 5	1.5 +/- 0.2
Selegiline (reference)	-	2.9	>200	88 +/- 4	5.1 +/- 0.7	58 +/- 6	85 +/- 5	1.4 +/- 0.2
6-OHDA only	-	-	-	47 +/- 6	-	100	48 +/- 5	4.1 +/- 0.5
Untreated control	-	-	-	100	-	-	100	1.0

Viability of retinoic acid-differentiated SH-SY5Y cells co-treated with 6-OHDA (100 uM, 24 h) and each hydrazone (10 uM pretreatment) across the series MO-1 to MO-7, alongside ascorbic acid (100 uM) and selegiline (10 uM) reference controls and the 6-OHDA-only and untreated conditions. Values are mean +/- SD, n = 3 independent experiments; viability is expressed as % of the untreated (no toxin, no compound) control.



The pattern that emerges from this series is not a surprising one in the abstract — ortho-dihydroxyphenyl (catechol) substitution outperforming a single phenol, which in turn outperforms an unsubstituted ring or an electron-withdrawing nitro group — but it is reassuring that it reproduces so cleanly inside a live-cell neurotoxicity assay rather than only in a cell-free radical assay. Catechol-type hydrazones can donate two sequential hydrogen atoms to a peroxyl radical and, after the first oxidation, delocalize the resulting semiquinone radical across the ring, and the same *ortho*-dihydroxy arrangement chelates the redox-active Fe^{2+}/Fe^{3+} that would otherwise drive Fenton generation of hydroxyl radical from the H_2O_2 that 6-OHDA auto-oxidation produces intracellularly. That combination — direct radical quenching plus iron sequestration — is exactly the mechanism proposed for aroylhydrazone-based iron chelators developed originally for iron-overload and antiproliferative indications, and it is a reasonable working explanation for why MO-3 outperformed every other member of this series on every endpoint we measured.

Where our results add something more specific is in the ROS/JC-1/caspase-3 correlation structure. If a hydrazone acted purely as an extracellular or membrane-level radical scavenger with no further downstream consequence, one would expect its ROS-suppressing potency to predict its effect on caspase-3 about as well as its effect on $\Delta\Psi m$. Instead we found caspase-3 protection tracking mitochondrial membrane potential preservation more tightly than it tracked ROS suppression per se, which fits the conventional intrinsic-apoptosis sequence — oxidative insult, mitochondrial permeabilization, cytochrome c release, caspase-3 activation — described for 6-OHDA and for nitric-oxide-induced death in this same cell background some years ago [21], and argues that at least part of what MO-3 and, to a lesser degree, MO-4 and MO-7 are doing is protecting the mitochondrion itself rather than simply scrubbing cytosolic radicals before they reach it.

The dimethylamino compound MO-5 is the one member of the series whose behavior does not fit neatly into a pure radical-scavenging story, and we think that is worth dwelling on rather than smoothing over. It has no phenolic hydrogen to donate, yet it produced meaningfully better protection on the mitochondrial and caspase readouts than its comparatively

unimpressive ROS-suppression would predict. Para-dialkylamino aryl systems are strong π-donors and can stabilize charge-transfer states that intercept certain radical species by electron transfer rather than classical hydrogen-atom transfer, and something structurally close to that behavior has been proposed for other aminoaryl hydrazones and Schiff bases with antioxidant activity that does not map cleanly onto simple phenolic content [18]. We are not in a position to assign a mechanism from a whole-cell assay panel, but MO-5's disproportionate mitochondrial and anti-caspase effect relative to its ROS numbers is the kind of internal inconsistency that a larger series or an isolated-mitochondria experiment could usefully chase.

At the other end, the near-total inactivity of the unsubstituted (MO-1) and nitro-substituted (MO-6) hydrazones is in line with what several groups working on pyrrole- and benzimidazole-based hydrazone neuroprotectants have reported: electron-withdrawing or non-donating aryl substituents essentially switch off the radical-scavenging function of the hydrazone core, even though the C=N-NH-C(=O) linkage itself is retained [9,10,13]. The small residual anti-caspase effect we saw with MO-6 despite its lack of antioxidant or viability benefit is a pattern that keeps recurring in this general chemical space — several isatin- and oxadiazole-hydrazone series with weak direct antioxidant activity have nonetheless shown measurable anti-apoptotic or MAO-inhibitory activity through mechanisms unrelated to radical scavenging [14,15] — and a plausible if unproven explanation here is a modest, MAO-independent interaction with the intrinsic apoptotic machinery itself rather than anything upstream of it.

Set against the wider hydrazone-neuroprotection literature, our EC50 values for the active compounds (7-14 μM for MO-3, MO-4 and MO-7) sit in a broadly comparable range to what has been reported for pyrrole-based hydrazide-hydrazones and benzimidazole arylhydrazones evaluated by largely the same MTT/DCFH-DA/JC-1 battery in SH-SY5Y cells challenged with 6-OHDA or related oxidative insults [11,10,12], and the magnitude of ROS suppression we observed with MO-3 (roughly 64% relative reduction) is very much in line with what has been reported for other catechol- or dihydroxyphenyl-bearing hydrazones tested directly on this cell line [17]. We would not claim any of our seven compounds is more potent than the best-performing members of those published series — direct cross-study comparison is always confounded by differences in toxin, exposure time, and differentiation protocol — but the internal consistency of the structure-activity trend, replicated across four mechanistically distinct endpoints in one experimental series, is the more useful contribution here than any single potency number.

There are limits worth stating plainly. SH-SY5Y, even retinoic-acid-differentiated, is not a dopaminergic neuron, and a chemical 6-OHDA insult delivered over 24 h is a caricature of the years-long, multifactorial process that produces nigral degeneration in a person; neither MAO-B inhibition, blood-brain-barrier permeability, nor in vivo pharmacokinetics were assessed for any compound in this series, and all of those would need to fall into place before MO-3 or its analogs could be considered anything more than a chemical starting point. We also did not directly measure iron-chelating capacity, which our mechanistic argument leans on; that would be a natural next experiment.

Seven new indole-3-ylacetohydrazide-derived aroylhydrazones were synthesized and evaluated side by side for cytotoxicity and for neuroprotection against 6-OHDA-induced oxidative injury in SH-SY5Y neuroblastoma cells, using viability, intracellular ROS, mitochondrial membrane potential, and caspase-3 activation as a coordinated four-endpoint readout. Neuroprotective potency tracked aryl substitution in a graded, chemically sensible way: the catechol derivative MO-3 was consistently the most protective compound across every endpoint, the vanillin-type and hindered-phenol analogs MO-4 and MO-7 were intermediate, the monophenol MO-2 was weakly active, and the unsubstituted and nitro-substituted hydrazones MO-1 and MO-6 were essentially without effect on viability, ROS, or mitochondrial integrity. The tighter correlation of caspase-3 protection with mitochondrial membrane potential than with ROS suppression alone points toward mitochondrial preservation, rather than cytosolic radical scavenging in isolation, as the more proximate event underlying protection in the more active compounds. MO-3, and to a lesser extent MO-4 and MO-7, represent reasonable candidates for follow-up work — iron-chelation assays, MAO-B screening, and eventually an in vivo Parkinsonian model — within the broader effort to find hydrazone-based neuroprotectants for oxidative, Parkinson's-disease-relevant neurodegeneration.

References

1. Chang KH, Chen CM (2020) The Role of Oxidative Stress in Parkinson's Disease. Antioxidants, 9(7):597, DOI:10.3390/antiox9070597.

2. Puspita L, Chung SY, Shim JW (2017) Oxidative stress and cellular pathologies in Parkinson's disease. Molecular Brain, 10:53, DOI:10.1186/s13041-017-0340-9.

3. Xicoy H, Wieringa B, Martens GJM (2017) The SH-SY5Y cell line in Parkinson's disease research: a systematic review. Molecular Neurodegeneration, 12:10, DOI:10.1186/s13024-017-0149-0.

4. Ioghen OC, Ceafalan LC, Popescu BO (2023) SH-SY5Y Cell Line In Vitro Models for Parkinson Disease Research-Old Practice for New Trends. Journal of Integrative Neuroscience, 22(1):20, DOI:10.31083/j.jin2201020.

5. Korecka JA, van Kesteren RE, Blaas E, Spitzer SO, Kamstra JH, Smit AB, Swaab DF, Verhaagen J, Bossers K (2013) Phenotypic characterization of retinoic acid differentiated SH-SY5Y cells by transcriptional profiling. PLoS ONE, 8(5):e63862, DOI:10.1371/journal.pone.0063862.

6. Ferlazzo N, Cirmi S, Maugeri A, Russo C, Lombardo GE, Gangemi S, Calapai G, Mollace V, Navarra M (2020) Neuroprotective Effect of Bergamot Juice in 6-OHDA-Induced SH-SY5Y Cell Death, an In Vitro Model of Parkinson's Disease. Pharmaceutics, 12(4):326, DOI:10.3390/pharmaceutics12040326.

7. Betharia S, Rondon-Ortiz AN, Brown DA (2019) Disubstituted Dithiolethione ACDT Exerts Neuroprotective Effects Against 6-Hydroxydopamine-Induced Oxidative Stress in SH-SY5Y Cells. Neurochemical Research, 44(8):1878-1892, DOI:10.1007/s11064-019-02823-3.

8. Hyon JY, Lee HJ, Yun SH, Han EH, Chung YH (2023) Comparative proteomics study of mitochondrial electron transport system modulation in SH-SY5Y cells following MPP+ versus 6-OHDA-induced neurodegeneration. Journal of Analytical Science and Technology, 14:1,

DOI:10.1186/s40543-022-00365-y.

9. Kondeva-Burdina M, Mateev E, Angelov B, Tzankova V, Georgieva M (2022) In Silico Evaluation and In Vitro Determination of Neuroprotective and MAO-B Inhibitory Effects of Pyrrole-Based Hydrazones: A Therapeutic Approach to Parkinson's Disease. Molecules, 27(23):8485, DOI:10.3390/molecules27238485.

10. Anastassova N, Aluani D, Hristova-Avakumova N, Tzankova V, Kondeva-Burdina M, Rangelov M, Todorova N, Yancheva D (2022) Study on the Neuroprotective, Radical-Scavenging and MAO-B Inhibiting Properties of New Benzimidazole Arylhydrazones as Potential Multi-Target Drugs for the Treatment of Parkinson's Disease. Antioxidants, 11(5):884, DOI:10.3390/antiox11050884.

11. Manov M, Stefanova D, Kondeva-Burdina M, Yordanov Y, Sharkov M, Tzankova D, Mateev E, Georgieva M, Popov G, Manov V, Frosini M, Valoti M, Tzankova V (2026) Neuroprotective and Antioxidant Activity of Newly Synthesized N-Pyrrolyl Hydrazide-Hydrazones in Experimental Models of Neurotoxicity In Vitro and In Vivo. International Journal of Molecular Sciences, 27(1):370, DOI:10.3390/ijms27010370.

12. Karatchobanov V, Mateev E, Valkova I, Kondeva-Burdina M, Georgieva M (2025) Novel Pyrrole-Based Hydrazide-Hydrazones: Synthesis, In Vitro Evaluation of Antioxidant and Neuroprotective Activity, In Silico ADME, and DFT Studies. Antioxidants, 15(6):666, DOI:10.3390/antiox15060666.

13. Georgieva M, Sharkov M, Mateev E, Tzankova D, Popov G, Manov V, Zlatkov A, Simeonova R, Kondeva-Burdina M (2025) Classical Paal-Knorr Cyclization for Synthesis of Pyrrole-Based Aryl Hydrazones and In Vitro/In Vivo Evaluation on Pharmacological Models of Parkinson's Disease. Molecules, 30(15):3154, DOI:10.3390/molecules30153154.

14. Kumar S, Oh JM, Prabhakaran P, Awasti A, Kim H, Mathew B (2024) Isatin-tethered halogen-containing acylhydrazone derivatives as monoamine oxidase inhibitor with neuroprotective effect. Scientific Reports, 14(1):1264, DOI:10.1038/s41598-024-51728-x.

15. Karabelyov V, Angelova VT, Sharkov M, Todorova N, Kondeva-Burdina M (2023) In vitro/in vivo effects of some new 2,5-disubstituted 1,3,4-oxadiazole and hydrazone analogues targeting Parkinson's disease. Journal of Molecular Structure, 1288:135755, DOI:10.1016/j.molstruc.2023.135755.

16. de Freitas Silva M, Cristancho Ortiz CJ, Coelho LF, et al. (2024) Synthesis and pharmacological evaluation of novel N-aryl-cinnamoyl-hydrazone hybrids designed as neuroprotective agents for the treatment of Parkinson's disease. Bioorganic Chemistry, 150:107587, DOI:10.1016/j.bioorg.2024.107587.

17. Tzankova D, Kuteva H, Mateev E, Stefanova D, Dzhemadan A, Yordanov Y, Mateeva A, Tzankova V, Kondeva-Burdina M, Zlatkov A, Georgieva M (2023) Synthesis, DFT Study, and In Vitro Evaluation of Antioxidant Properties and Cytotoxic and Cytoprotective Effects of New Hydrazones on SH-SY5Y Neuroblastoma Cell Lines. Pharmaceuticals, 16(9):1198, DOI:10.3390/ph16091198.

18. Omidi S, Kakanejadifard A (2020) A review on biological activities of Schiff base, hydrazone, and oxime derivatives of curcumin. RSC Advances, 10(50):30186-30202, DOI:10.1039/D0RA05720G.

19. Mosmann T (1983) Rapid colorimetric assay for cellular growth and survival: application to proliferation and cytotoxicity assays. Journal of Immunological Methods, 65(1-2):55-63, DOI:10.1016/0022-1759(83)90303-4.

20. Perelman A, Wachtel C, Cohen M, Haupt S, Shapiro H, Tzur A (2012) JC-1: alternative excitation wavelengths facilitate mitochondrial membrane potential cytometry. Cell Death & Disease, 3:e430, DOI:10.1038/cddis.2012.171.

21. Uehara T, Kikuchi Y, Nomura Y (1999) Caspase activation accompanying cytochrome c release from mitochondria is possibly involved in nitric oxide-induced neuronal apoptosis in SH-SY5Y cells. Journal of Neurochemistry, 72(1):196-205, DOI:10.1046/j.1471-4159.1999.0720196.x.